FIAS: FEATURE IMBALANCE-AWARE MEDICAL IMAGE SEGMENTATION WITH DYNAMIC FUSION AND MIXING ATTENTION

Xiwei Liu[1] *Min Xu*[2] *Qirong Ho*[1]

[1] Mohamed bin Zayed Univeristy of Artificial Intelligence, [2]Carnegie Mellon University

ABSTRACT

With the growing application of transformer in computer vision, hybrid architecture that combine convolutional neural networks (CNNs) and transformers demonstrates competitive ability in medical image segmentation. However, direct fusion of features from CNNs and transformers often leads to feature imbalance and redundant information. To address these issues, we propose a Feaure Imbalance-Aware Segmentation (FIAS) network, which incorporates a dual-path encoder and a novel Mixing Attention (MixAtt) decoder. The dual-branches encoder integrates a DilateFormer for long-range global feature extraction and a Depthwise Multi-Kernel (DMK) convolution for capturing fine-grained local details. A Context-Aware Fusion (CAF) block dynamically balances the contribution of these global and local features, preventing feature imbalance. The MixAtt decoder further enhances segmentation accuracy by combining self-attention and Monte Carlo attention, enabling the model to capture both small details and large-scale dependencies. Experimental results on the Synapse multi-organ and ACDC datasets demonstrate the strong competitiveness of our approach in medical image segmentation tasks.

Index Terms— Medical image segmentation, Transformer, Convolutional neural networks, Attention mechanism

1. INTRODUCTION

Convolutional neural networks (CNNs),particularly U-shaped architectures like U-Net, have become the representative network for medical image segmentation due to their effective encoder-decoder pyramid structure. However, CNNs inherently struggle to capture global context because of the local nature of convolution operations. Vision Transformer (ViT) [1], leveraging self-attention mechanisms, excel in modeling long-range dependencies, but despite outperforming CNNs in many tasks, transformers still face challenges in capturing fine-grained local details essential for precise segmentation.

Recently, several studyies [2][3][4][5] have focused on hybrid architectures that combine the local feature extraction ability of CNNs with the global context modeling strength of transformers. For example, TransUnet [6] incorporates a transformer layer into a CNN encoder to capture global dependencies. UNETR [4] and ConvTransSeg [7] utilize CNN and transformer components either as separate encoders or decoders. CATS [2] combines a CNN and transformer as dual-branches encoders. MIST [8] adopt MaxViT [9] in the encoder and a convolutional attention mixing decoder to capture both short- and long-range dependencies across spatial dimensions. Similarly, E-TransUNet [10] integrate an enhanced Res2Net module into the encoder to improve feature extraction capabilities.

Despite these advancements, existing methods likes [2][3] typically fuse local CNN features and global transformer features through simple operations such as summation or concatenation. However, these method has key limitations: (1) The relative importance of local and global features can vary, and simple fusion can lead to feature imbalance, where critical local or global information may be either overshadowed or overemphasized. (2) Direct concatenation or summation overlooks the interactions between multi-scale features, often resulting in redundant or conflicting information. This imbalance between global and local features particularly affects the model's ability to accurately capture both fine-grained details (e.g., small targets) and larger semantic structures, which is critical in complex medical image segmentation tasks. Considering these limitation, we develop FIAS, a novel segmentation framework that combines a DilateFormer [11] and Depthwise Multi-Kernel (DMK) convolution as dual-path encoders, along with a Context-Aware Fusion (CAF) block for dynamic feature fusion and a Mixing Attention (MixAtt) decoder.

Our contributions are threefold:

• We propose a CAF block, which dynamically fuses global and local features based on their relevance across different scales. By intelligently adjusting the contributions from each encoder, CAF ensures balanced feature fusion, avoiding redundancy and information loss.

• We develop a novel MixAtt decoder that enhances the network's ability to exploit cross-scale correlations. By combining self-attention with Monte Carlo attention, MixAtt captures both short-range and long-range dependencies, improving the segmentation of both small objects and larger anatomical structures.

• We validate FIAS on the Synapse and ACDC datasets through extensive experiments, exhibiting superior performance over other medical image segmentation methods.

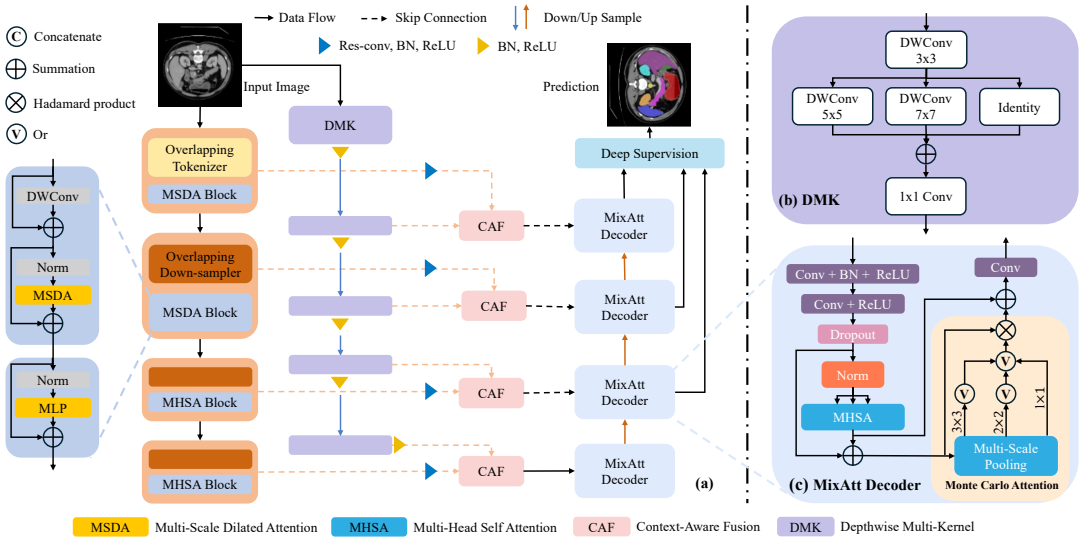

Fig. 1: (a) Overview of the proposed network architecture with dual-branches encoders: a DilateFormer encoder and a Depthwise Multi-Kernel (DMK) convolution encoder, fused via a Context-Aware Fusion (CAF) block. (b) Detailed design of the DMK convolution encoder, featuring multi-scale depthwise convolutions. (c) The Mixing Attention (MixAtt) decoder, combining self-attention and Monte Carlo attention mechanisms. Refer to Section 2 for details.

2. METHODS

2.1. Framwork Overview

The proposed FIAS framework, shown in Fig. 1, consists of dual-branches encoder: a pre-trained DilateFormer and a DMK convolution encoder, along with the novel MixAtt decoder. The CAF dynamically fuses multi-scale features from both encoders, ensuring balanced representation.The model also incorporates a deep supervision strategy to enhance optimization and facilitate better learning at multiple levels.

2.2. Network Components

DilateFormer Encoder. The DilateFormer [11] is a hierarchical transformer that serves as one of the core encoders in our framework, designed for efficient modeling of both local and global semantic information across multiple scales. It consists of Multi-Scale Dilated Attention (MSDA) blocks in the first two low-level stages, followed by Multi-Head Self-Attention (MHSA) [12] blocks in the higher-level stages (with 2, 2, 6, and 2 blocks, respectively). The MSDA [11] blocks combine depthwise convolution (DWConv), sliding window dilated attention (SWDA), and multi-layer perceptron (MLP) modules. By using varying dilation rates in different layers, the DilateFormer maintains the ability to process global information while also improving the capture of fine-grained local details, making it ideal for tasks requiring both long-range dependencies and high-resolution spatial information.

DMK Encoder. The Depthwise Multi-Kernel (DMK) convolution is an inception-style module [13] designed to capture both local and multi-scale contextual information. It first applies a small kernel convolution to grasp local features, followed by a series of parallel depthwise convolutions to capture multi-scale context. Mathematically, the operation of the DMK block at the l-stage is represented as:

$$\begin{aligned} \boldsymbol{L}_l &= \texttt{Conv}_{k_s \times k_s}(\boldsymbol{X}_{l-1}) \\ \boldsymbol{Z}_l^{(m)} &= \texttt{DWConv}_{k^{(m)} \times k^{(m)}}(\boldsymbol{L}_{l-1}), \quad m = 1, 2. \end{aligned} \tag{1}$$

Here, $\boldsymbol{L}_l$ denotes the local feature extracted by $k_s \times k_s$ convolution, and $\boldsymbol{Z}_l^{(m)}$ is the multi-scale context feature extracted by the m-th $k^{(m)} \times k^{(m)}$ depthwise convolution (DWConv). In our method, we set $k_s = 3$ and $k^{(m)} = (m+1) \times 2 + 1$. Then, the multi-scale local features are fused using a 1×1 convolution, characterizing the interrelations among various channels.

$$\boldsymbol{F}_l = \texttt{Conv}_{1\times1}(\boldsymbol{L}_l + \sum_{m=1}^{2} \boldsymbol{Z}_l^{(m)}) \tag{2}$$

where $\boldsymbol{F}_l$ represents the output feature of DMK at l-th stage.

Context-Aware Fusion. We propose a Context-Aware Fusion (CAF) module aimed at dynamically fusing global and local features extracted from both DilateFormer and DMK encoders, addressing imbalance and avoiding redundant information. As illustrated in Fig. 2, the fusion process begins by reducing the number of channels using global channel information w_{ch}, ensuring that only the most relevant features are retained. The operation $\texttt{E}_{ch}$ to extract w_{ch} from feature maps $\boldsymbol{F}_1$ and $\boldsymbol{F}_2$ is defined as follow:

$$\begin{aligned} E_{ch}(\cdot) &= \sigma(\texttt{Conv}(\texttt{Cat}(\mathcal{P}_{avg}(\texttt{Conv}(\cdot)), \mathcal{P}_{map}(\texttt{Conv}(\cdot))))) \\ w_{ch} &= E_{ch}([\boldsymbol{F}_1; \boldsymbol{F}_2]) \end{aligned} \tag{3}$$

where σ is Sigmoid activation function, $\texttt{Cat}$ is concatenation, $\mathcal{P}_{avg}$ and $\mathcal{P}_{map}$ represents average and max pooling, respectively. The global channel information w_{ch} is then used to

recalibrate the fused features, helping the model to prioritize important channels while suppressing less informative ones:

$$\boldsymbol{F}' = \texttt{Conv}(w_{ch} \otimes [\boldsymbol{F}_1; \boldsymbol{F}_2]) \quad (4)$$

To model the spatial-wise inter-dependencies among feature maps, we compute the global spatial information w_{sp}, which is used to calibrate feature maps and facilitate the emphasis on salient spatial regions.

$$w_{sp} = \sigma(\texttt{Conv}(\mathcal{P}_{avg}(\texttt{Conv}(\boldsymbol{F}_1) \oplus \texttt{Conv}(\boldsymbol{F}_2)))) \quad (5)$$

$$\hat{\boldsymbol{F}} = w_{sp} \otimes \boldsymbol{F}' \quad (6)$$

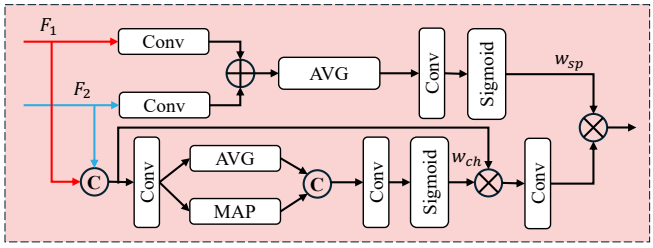

Fig. 2: The architecture of the CAF module.

MixAtt Decoder. The novel Mixing Attention (MixAtt) decoder employs a mixing-attention strategy, combining self-attention and Monte Carlo attention (MCA) [14] to capture both global dependencies and fine-grained details at various stages. At stage l, $\boldsymbol{P}_{l-1}$ from previous decoder stage and fused feature $\boldsymbol{F}_l$ from CAF is concatenated and passed through convolution, which extracts the relevant salient features and reduce the channel dimension by half:

$$\boldsymbol{P}_l^1 = \texttt{D}(\texttt{R}(\texttt{Conv}(\texttt{R}(\texttt{BN}(\texttt{Conv}(\texttt{Cat}(\boldsymbol{P}_{l-1}, \hat{\boldsymbol{F}}_l)))))) \quad (7)$$

where D, R, BN refers to dropout, ReLU activation function and batch normalization, respectively. This operation ensures that the input features are well-prepared for the subsequent attention mechanisms by normalizing and reducing redundancy. Then, MHSA [12] is applied, where the number of attention heads decreases progressively across the decoder blocks (8, 6, 4, and 2, respectively). The output of the MHSA is then combined with the input through a skip connection:

$$\boldsymbol{P}_l^2 = \texttt{MHSA}(\texttt{norm}(\boldsymbol{P}_l^1)) + \boldsymbol{P}_l^1 \quad (8)$$

where norm denotes the layer normalization. Then, we apply MCA to the features $\boldsymbol{P}_l^2$. MCA uses a random-sampling-based pooling operation to generate scale-agnostic attention maps, which enhance the network's ability to exploit cross-scale correlations and identify small objects in medical images. MCA generate attention maps at multiple scales (3×3, 2×2, and 1×1). However, only a 1×1 attention map, randomly selected from these three pooled scales, is used, which is computed as follows:

$$\mathcal{A} = \sum_{i=1}^{3} m_i \mathcal{P}_{avg}^{(i)}(\boldsymbol{P}_l^2) \quad (9)$$

where i indicates the scale of the output attention map, and m_i represents the association probability, which satisfies the conditions $\sum_{i=1}^{3} m_i = 1$ and $\prod_{i=1}^{3} m_i = 0$. This ensures the attention maps are scale-agnostic and generalizable across different scales. Finally, we perform attention aggregation and mixing, where MHSA and MCA are added together:

$$\boldsymbol{P}_l = \texttt{Conv}((\boldsymbol{P}_l^2 \otimes \mathcal{A}) \oplus \texttt{MHSA}(\texttt{norm}(\boldsymbol{P}_l^1))) \quad (10)$$

2.3. Loss Function

To ensure that intermediate layers contribute to the learning process, we use the outputs from the last three MixAtt decoder blocks for deep supervision [15]. This strategy helps guide the model in capturing meaningful features across multiple levels, enhancing both fine-grained details and broader semantic information. To further improve feature representation, we incorporate a feature mixing strategy [16] that generates $2^n - 1 = 7$ non-empty subsets from the n=3 decoder prediction maps. These subsets are aggregated to produce the final prediction map used for loss calculation. This multi-scale approach allows the model to capture both local details and global context, improving segmentation accuracy.

For loss computation, we apply DICE (L_{DICE}) and CrossEntropy (L_{CE}) loss to all 7 individual prediction maps and their corresponding ground truth masks to estimate the losses. We aggregate all estimated losses using the following function to compute the final loss:

$$L_{total} = \gamma L_{DICE} + (1 - \gamma) L_{CE} \quad (11)$$

In our experiments, we set $\gamma = 0.4$.

3. EXPERIMENTS AND RESULTS

3.1. Datasets and Implementation Details

We evaluate our proposed method on two public datasets, using the average Dice Similarity Coefficient (DSC) and the 95% Hausdorff Distance (HD95) as evaluation metrics to assess segmentation accuracy and boundary alignment.

Synapse multi-organ segmentation dataset (Synapse)[1] is a multi-organ dataset, includes 30 abdominal CT scans with 18 for training and 12 for validation. It contains segmentation masks for eight organs including the aorta, gallbladder, right kidney, left kidney, liver, pancreas, spleen, and stomach.

Automatic Cardiac Diagnosis Challenge (ACDC)[2] contains 100 cardiac MRI scans, with multiple 2D slices featuring three organs: right ventricle (RV), myocardium (MYO), and left ventricle (LV). Following the setting in [6], 70 cases are used for training, 10 for validation and 20 for testing.

Implementation details. Our method is implemented by Pytorch v1.8.0 with a GeForce RTX 4090 GPU. We use Adam optimizer with a learning rate 0.0001 and weight decay of 0.0001. The training batch size was set 2 for all experiments. The input images are resized to $256 * 256$, and we apply data augmentation techniques such as rotation, zoom, horizontal and vertical shifting, and flipping to improve generalization.

3.2. Results

Quantitative result. To demonstrate the effectiveness of our proposed FIAS method, we compared it with several state-of-the-art hybrid CNN-Transformer on both datasets. The

[1] https://www.synapse.org/#!Synapse:syn3193805/wiki/217789

[2] https://www.creatis.insa-lyon.fr/Challenge/ acdc/

Table 1: Performance comparison on the Synapse Dataset for organ segmentation. Higher mean DSC values indicating better performance. Lower HD95 scores represent more accurate boundary matching. Best results are highlighted in bold.

Methods	Organs								Average	
	Aorta	Gallbladder	Kidney(L)	Kidney(R)	Liver	Pancreas	Spleen	Stomach	HD95 ↓	DSC ↑
TransUNet [6]	87.23	63.13	81.87	77.02	94.08	55.86	88.05	75.62	31.69	77.48
UNETR [4]	89.80	56.30	85.60	84.521	94.57	60.47	85.00	70.46	18.59	78.35
Swin-UNet [17]	85.47	64.66	82.89	74.92	94.29	56.58	89.06	76.60	21.55	79.13
TransUNet+ [18]	88.70	67.57	82.48	81.42	94.20	65.73	90.55	81.95	20.16	81.57
AFTer-UNet [19]	**90.91**	64.81	87.90	85.30	92.20	63.54	90.99	72.48	20.83	81.02
MT-UNet [20]	87.92	64.99	81.47	77.29	93.06	59.46	87.75	76.81	26.59	78.59
E-TransUNet [10]	87.41	67.34	85.95	82.88	**95.11**	66.53	90.01	83.49	19.42	82.34
MIST [8]	89.15	74.58	93.28	92.54	94.94	72.43	**92.83**	87.23	11.07	86.92
FIAS (Ours)	90.47	**76.31**	**94.79**	**92.84**	94.93	**72.56**	91.43	**89.12**	**8.75**	**87.81**

quantitative results on the Synapse dataset are shown in Table 1. After conducting the experiments five times, our model achieved an average DSC of 89.06±0.1 and an average HD95 of 7.75±0.1. Among the eight organs, our method achieves average DSC to optimal values in Gallbladder, Kidney(L)(R), Pancreas and Stomach. High average DSC levels were also obtained in the other three organs. For the ACDC dataset, the quantitative results are presented in Table 2. The average DSC 93.27±0.1 of our method performed best on all three sites. The experimental results show that our proposed method exhibits competitive performance compared to other methods.

Table 2: Comparative quantitative analysis on ACDC.

Models	Mean DSC ↑	RV	MYO	LV
TransUNet [6]	89.71	88.86	84.53	95.73
UNETR [4]	86.61	85.29	86.52	94.02
SwinUNet [17]	90.00	88.55	85.62	95.83
TransUNet+ [18]	90.42	89.15	87.65	94.12
AFTer-UNet [19]	90.82	87.42	89.31	95.73
MT-UNet [20]	90.43	86.64	89.04	95.62
E-TransUNet [10]	91.64	90.21	89.12	95.61
MIST [8]	92.56	91.23	90.31	96.14
FIAS (Ours)	**93.27**	**92.09**	**91.25**	**96.47**

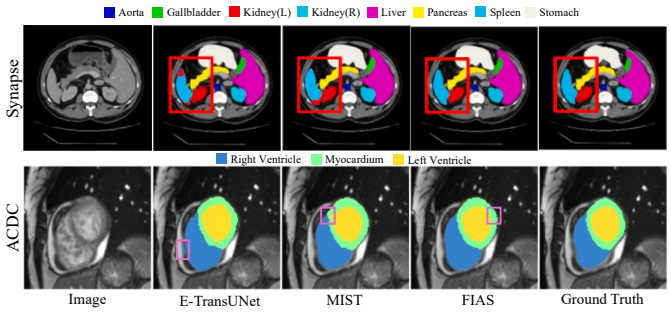

Fig. 3: Qualitative comparison on the Synapse and ACDC dataset. We compare our FIAS with MIST and E-TransUNet.

Qualitative Visualization. Fig. 3 presents a visual comparison of the segmentation results from FIAS, MIST, and E-TransUNet, along with the ground truth. Our model, FIAS, consistently avoids the common pitfalls of either missing small structures or producing overly coarse segmentations, particularly in regions where other models either over-segment or fail to capture the precise boundaries. The MixAtt decoder s key to this performance, as it integrates self-attention and MCA, enabling the model to focus on both fine-grained local features and the broader contextual structure. This balanced representation helps the model effectively capture the semantic dependencies between adjacent regions, which is critical for complex organ structures.

3.3. Ablation study

To further demonstrate the effectiveness of each component of our method, we conducted an ablation study on the ACDC dataset, as summarized in Table 3. By altering key components like the DMK encoder, CAF block, and MixAtt decoder, we observe a significant drop in both DSC and HD95. This demonstrates the dynamic fusion of features is essential for balancing global and local context, and highlight the importance of attention mechanisms in decoder in capturing multi-scale dependencies and improving segmentation precision.

Table 3: Analysis of ablation study on network components.

DMK	Feature Fusion	MixAtt	HD95 ↓	DSC ↑
-	CAF	✓	11.47	86.53
✓	Summation	✓	14.22	84.89
✓	CAF	-	19.73	82.68
✓	CAF	✓	**8.75**	**87.81**

4. CONCLUSION

In this paper, we proposed FIAS, a novel hybrid CNN-Transformer segmentation framework to address feature imbalance. The CAF block dynamically fuses global and local features, while the MixAtt decoder captures cross-scale dependencies. Experiments on the Synapse and ACDC datasets demonstrate that FIAS performs competitively compared to other state-of-the-art methods in both accuracy and boundary precision, particularly in challenging medical image segmentation tasks.

5. REFERENCES

[1] Alexey Dosovitskiy, "An image is worth 16x16 words: Transformers for image recognition at scale," *arXiv preprint arXiv:2010.11929*, 2020.

[2] Hao Li, Dewei Hu, Han Liu, Jiacheng Wang, and Ipek Oguz, "Cats: complementary cnn and transformer encoders for segmentation," in *2022 IEEE 19th International Symposium on Biomedical Imaging (ISBI)*. IEEE, 2022, pp. 1–5.

[3] Hao Li, Han Liu, Dewei Hu, Xing Yao, Jiacheng Wang, and Ipek Oguz, "Cats v2: hybrid encoders for robust medical segmentation," in *Medical Imaging 2024: Image Processing*. SPIE, 2024, vol. 12926, pp. 130–137.

[4] Ali Hatamizadeh, Yucheng Tang, Vishwesh Nath, Dong Yang, Andriy Myronenko, Bennett Landman, Holger R Roth, and Daguang Xu, "Unetr: Transformers for 3d medical image segmentation," in *Proceedings of the IEEE/CVF winter conference on applications of computer vision*, 2022, pp. 574–584.

[5] Yundong Zhang, Huiye Liu, and Qiang Hu, "Transfuse: Fusing transformers and cnns for medical image segmentation," in *Medical image computing and computer assisted intervention–MICCAI 2021: 24th international conference, Strasbourg, France, September 27–October 1, 2021, proceedings, Part I 24*. Springer, 2021, pp. 14–24.

[6] Jieneng Chen, Yongyi Lu, Qihang Yu, Xiangde Luo, Ehsan Adeli, Yan Wang, Le Lu, Alan L Yuille, and Yuyin Zhou, "Transunet: Transformers make strong encoders for medical image segmentation," *arXiv preprint arXiv:2102.04306*, 2021.

[7] Zhendi Gong, Andrew P French, Guoping Qiu, and Xin Chen, "Convtransseg: A multi-resolution convolution-transformer network for medical image segmentation," *arXiv preprint arXiv:2210.07072*, 2022.

[8] Md Motiur Rahman, Shiva Shokouhmand, Smriti Bhatt, and Miad Faezipour, "Mist: Medical image segmentation transformer with convolutional attention mixing (cam) decoder," in *Proceedings of the IEEE/CVF Winter Conference on Applications of Computer Vision*, 2024, pp. 404–413.

[9] Zhengzhong Tu, Hossein Talebi, Han Zhang, Feng Yang, Peyman Milanfar, Alan Bovik, and Yinxiao Li, "Maxvit: Multi-axis vision transformer," in *European conference on computer vision*. Springer, 2022, pp. 459–479.

[10] Zijun Zhang, Xuanheng Li, Xiaohong Ma, and Yi Sun, "E-transunet: Enhanced transunet for medical image segmentation," in *2024 IEEE International Symposium on Biomedical Imaging (ISBI)*. IEEE, 2024, pp. 1–5.

[11] Jiayu Jiao, Yu-Ming Tang, Kun-Yu Lin, Yipeng Gao, Andy J Ma, Yaowei Wang, and Wei-Shi Zheng, "Dilateformer: Multi-scale dilated transformer for visual recognition," *IEEE Transactions on Multimedia*, vol. 25, pp. 8906–8919, 2023.

[12] A Vaswani, "Attention is all you need," *Advances in Neural Information Processing Systems*, 2017.

[13] Weihao Yu, Pan Zhou, Shuicheng Yan, and Xinchao Wang, "Inceptionnext: When inception meets convnext," in *Proceedings of the IEEE/CVF Conference on Computer Vision and Pattern Recognition*, 2024, pp. 5672–5683.

[14] Wei Dai, "Svanet: A scale-variant attention-based network for small medical object segmentation," *arXiv preprint arXiv:2407.07720*, 2024.

[15] Chen-Yu Lee, Saining Xie, Patrick Gallagher, Zhengyou Zhang, and Zhuowen Tu, "Deeply-supervised nets," in *Artificial intelligence and statistics*. Pmlr, 2015, pp. 562–570.

[16] Md Mostafijur Rahman and Radu Marculescu, "Multi-scale hierarchical vision transformer with cascaded attention decoding for medical image segmentation," in *Medical Imaging with Deep Learning*. PMLR, 2024, pp. 1526–1544.

[17] Hu Cao, Yueyue Wang, Joy Chen, Dongsheng Jiang, Xiaopeng Zhang, Qi Tian, and Manning Wang, "Swin-unet: Unet-like pure transformer for medical image segmentation," in *European conference on computer vision*. Springer, 2022, pp. 205–218.

[18] Yuhang Liu, Han Wang, Zugang Chen, Kehan Huangliang, and Haixian Zhang, "Transunet+: Redesigning the skip connection to enhance features in medical image segmentation," *Knowledge-Based Systems*, vol. 256, pp. 109859, 2022.

[19] Xiangyi Yan, Hao Tang, Shanlin Sun, Haoyu Ma, Deying Kong, and Xiaohui Xie, "After-unet: Axial fusion transformer unet for medical image segmentation," in *Proceedings of the IEEE/CVF winter conference on applications of computer vision*, 2022, pp. 3971–3981.

[20] Hongyi Wang, Shiao Xie, Lanfen Lin, Yutaro Iwamoto, Xian-Hua Han, Yen-Wei Chen, and Ruofeng Tong, "Mixed transformer u-net for medical image segmentation," in *ICASSP 2022-2022 IEEE international conference on acoustics, speech and signal processing (ICASSP)*. IEEE, 2022, pp. 2390–2394.